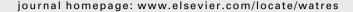


Available at www.sciencedirect.com







Electrosorptive desalination by carbon nanotubes and nanofibres electrodes and ion-exchange membranes

Haibo Li, Yang Gao, Likun Pan*, Yanping Zhang, Yiwei Chen, Zhuo Sun

Engineering Research Center for Nanophotonics & Advanced Instrument, Ministry of Education, Department of Physics, East China Normal University, Shanghai 200062, China

ARTICLE INFO

Article history:
Received 8 July 2008
Received in revised form
6 September 2008
Accepted 16 September 2008
Published online 2 October 2008

Keywords:
Electrosorption
Carbon nanotubes and nanofibres
Capacitive deionization
Ion-exchange membrane

ABSTRACT

A novel membrane capacitive deionization (MCDI) device, integrating both the advantages of carbon nanotubes and carbon nanofibers (CNTs–CNFs) composite film and ion-exchange membrane, was proposed with high removal efficiency, low energy consumption and low cost. The CNTs–CNFs film was synthesized by low pressure and low temperature thermal chemical vapor deposition. Several experiments were conducted to compare desalination performance of MCDI with capacitive deionization (CDI), showing that salt removal of the MCDI system was 49.2% higher than that of the CDI system. The electrosorption isotherms of MCDI and CDI show both of them follow Langmuir adsorption, indicating no change in adsorption behavior when ion-exchange membranes are introduced into CDI system. The better desalination performance of MCDI than that of CDI is due to the minimized ion desorption during electrosorption.

© 2008 Elsevier Ltd. All rights reserved.

1. Introduction

Capacitive deionization (CDI), as a typical application of electrosorption, is a powerful deionization technology that removes deleterious metal ions without high power consumption and secondary pollution with other conventional approaches. It has been developed as a potential technology for removing inorganic ions from aqueous solutions (Qi et al., 2007; Hou et al., 2006; Gabelich et al., 2002; Johnson and Newman, 1971; Xu et al., 1983; Matlosz and Newman, 1986; Welgemoed and Schutte, 2005; Zou et al., 2007). The principle of CDI is based on imposing an external electrostatic field between the electrodes in order to force charged ions to move towards oppositely charged electrodes. The charged ions can be attracted within the electrical double layer formed between the solvent and electrode interface.

Carbon materials of porous structure constitute very attractive electrodes for CDI processes because of their high

specific surface area and their good electrical conductivity (Pekala et al., 1998). Activated carbons (ACs) are the electrode materials that are used most frequently in CDI, but have several intrinsic disadvantages (Qu and Shi, 1998), such as low conductivity and irregular pore structures that result in limited electrosorption capacity. Thus, the most effective way to improve CDI performance is to develop new electrode materials with high conductivity and regular pore structures, such as carbon aerogels (Fang and Binder, 2006; Hwang and Hyun, 2004) and nanoporous carbons (Oh et al., 2006). Carbon nanotube (CNTs), due to their high ratio of surface area to volume and other outstanding properties, are suitable to be used as electrodes for CDI, which has been described in our previous studies (Wang et al., 2006; Gao et al., 2007).

During conventional CDI, when an electric potential is applied to electrodes, ions move from solution to electrode surfaces and are adsorbed on them. However, due to the attraction from ions with opposite charge near the electrode,

^{*} Corresponding author. Tel.: +86 021 62232420; fax: +86 021 62233897. E-mail address: lkpan@phy.ecnu.edu.cn (L. Pan).

ions that have been adsorbed on the electrode may be removed to the aqueous solution again. It means that ion adsorption and ion desorption occur simultaneously on the electrodes in CDI, which will affect seriously electrosorption capacity. To solve this problem, ion-exchange membranes, which have been widely used as a separation membranes can be introduced into the CDI system. The cation-exchange and anion-exchange membranes are selectively permeable to cations and anions, respectively. When they are applied with the electrodes in the electrosorption system, the ions with opposite charge will be prevented from moving towards the electrode. The ion desorption caused by the attraction from ions with opposite charge in the solutions will be minimized. Furthermore, the pore space near the electrode previously occupied by the ions with opposite charge can be freed to facilitate the ions to move towards electrode surface. Thus the salt removal capability can be enhanced. Jae-Bong Lee first introduced the ion-exchange membrane into CDI process (Lee et al., 2006). In their work, ion-exchange membranes were incorporated with activated carbon cloth, named as membrane capacitive deionization system (MCDI), to perform the desalination of power plant wastewater and the salt removal of sodium ions by MCDI was 19% higher than that by CDI.

In this work, low pressure and low temperature thermal chemical vapor deposition (CVD) has been carried out for large area synthesis of carbon nanotubes and nanofibres (CNTs-CNFs) composite films as CDI electrodes. Ion-exchange (cation-exchange and anion-exchange) membranes were introduced into CDI and the desalination performance and electrosorption isotherm of MCDI were investigated.

2. Experimental

2.1. Preparation of CNTs-CNFs composite film electrodes

The low pressure and low temperature thermal CVD system (Shanghai Nanoking Co.) was used to fabricate CNTs–CNFs composite film electrodes. Acetylene was used as the carbon feedstock and hydrogen as the carrier/dilution gas. The growth pressure was 20 kPa. The flow rate of acetylene and hydrogen was fixed at 50 and 100 sccm, respectively. The CNTs–CNFs growth was carried out for 30 min at a temperature of 550 °C. Conductive plates (graphite coated with nickel by sputtering) were used as substrates. Each conductive plate

was 70 mm wide \times 80 mm long \times 0.3 mm thick, and has a flow-through hole with the diameter of 6 mm. The thickness of CNTs–CNFs composite films was about 0.55 mm. The CNTs–CNFs composite films were grown directly and firmly anchored on the supporting conductive plate (current collector). Therefore, the monolithic forms and simultaneous combination of current collector and CNTs–CNFs composite films were realized. Good electrical connection to external power supply is ensured without weight loss and surface area reduction. The as-grown CNTs–CNFs film electrodes were immersed into 1 M HCl solution to get rid of Ni catalyst to avoid the influence of Ni during the electrosorption.

2.2. Charaterization of CNTs-CNFs composite film

The surface morphology and structure of CNTs-CNFs composite film were examined by JEOL JSM-LV5610 scanning electron microscopy (SEM), and Raman spectroscopy (Renishaw inVia). The pore size distribution of the CNTs-CNFs composite film are deduced from the N2 physical adsorption measurement data which were obtained with ASAP 2010 Accelerated Surface Area and Porosimetry System (Micrometitics, Norcross, GA).

2.3. Ion-exchange membranes

The ion-exchange membranes (Shanghai Chemistry, China) were used to adsorb the ions selectively on the electrodes. The cation-exchange membrane (15 Ω/m^2 , 70 mm wide \times 80 mm long \times 0.4 mm thick) is selectively permeable to cations and the anion-exchange membrane (20 Ω/m^2 , 70 mm wide \times 80 mm long \times 0.4 mm thick) is selectively permeable to anions. Their main characteristics are shown in Table 1.

2.4. Electrosorption unit cell setup

The electrosorption unit cell shown in Fig. 1(a) was employed. The assembly of one half of the unit cell is in the order: retaining plate/rubber gasket/electrode/ion-exchange membrane/rubber spacer/nylon spacer. Retaining plate was made of polymethyl methacrylate. The spacing of 1 mm between the electrodes was maintained by rectangular nylon spacer and a rubber spacer.

Table 1 – Main characteristic of ion-exchange membranes (cation-exchange and anion-exchange membranes)				
	Cation-exchange membrane	Anion-exchange membrane		
Thickness (mm)	0.4	0.4		
Resistance of membrane surface (Ω -cm ²)	15	20		
Chemistry stability (pH)	1–10	1–10		
Selective penetration (%)	90	89		
Permeability of water (ml/h cm ²)	0.2	0.2		
Heat stability (°C)	40	40		

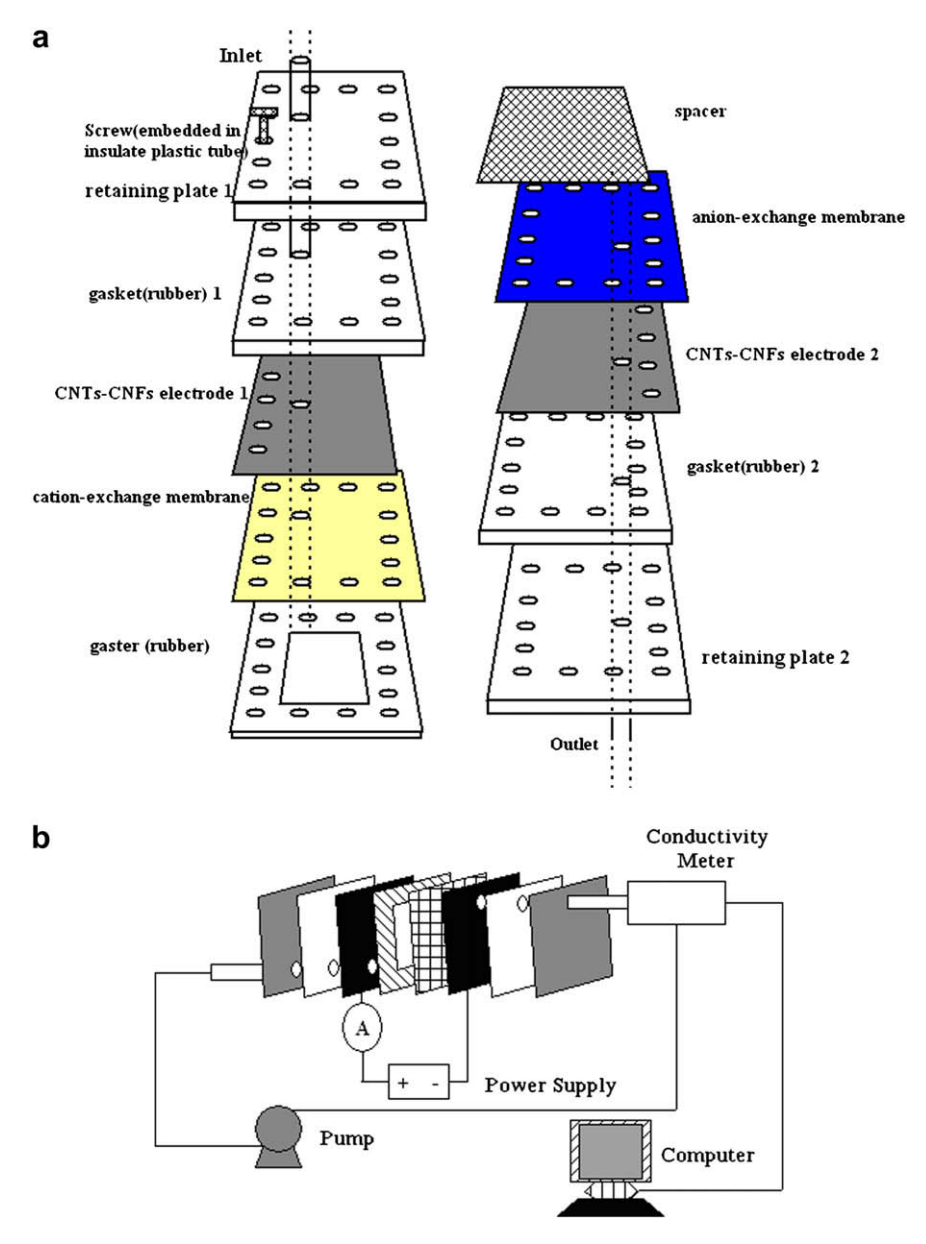


Fig. 1 - (a) Diagram of MCDI unit cell. (b) A continuously recycling system with an electrosorption unit cell.

2.5. Batch-mode electrosorption experiments

To investigate the total electrosorption capacity of MCDI system, batch-mode experiments were conducted in a continuously recycling system including an electrosorption unit cell. In each experiment, the solution was continuously pumped with a peristaltic pump into the cell and the effluent returned to the unit cell. The solution temperature was kept at 298 K and a flow rate around 40 ml/min was applied. Analytical grade sodium chloride (NaCl) was used for the aqueous solutions and a direct voltage of 0.6–1.6 V was applied. The relationship between conductivity and concentration was obtained according to a calibration table made prior to the experiment. The concentration variation of NaCl solution was continuously monitored and measured at the outlet of the unit cell using an ion conductivity meter, as shown in Fig. 1(b).

In our experiment, the salt removal is defined as follows:

Salt removal (%) =
$$\frac{C - C_0}{C} \times 100$$
 (1)

where C is initial conductivity and C_0 is the final conductivity.

3. Results and discussion

3.1. Morphology and structure of CNTs-CNFs composite films

Fig. 2 shows the surface morphologies of CNTs-CNFs composite films examined by SEM. The diameter of CNTs-CNFs which serve as the frame for the growing of CNTs is around 10–50 nm. The CNFs-CNTs are randomly entangled

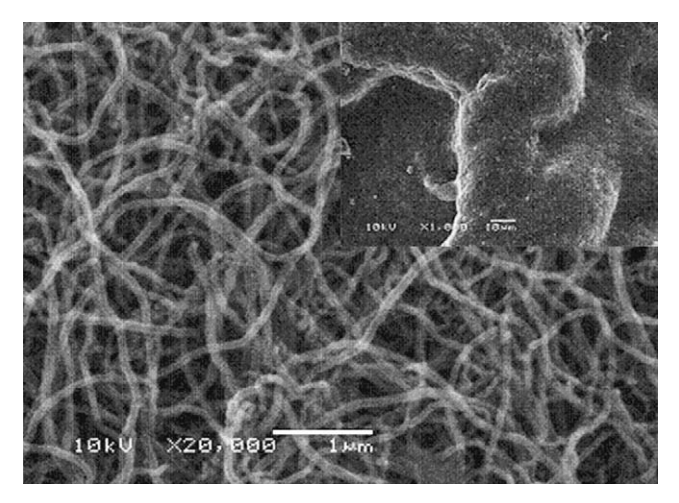


Fig. 2 – SEM image of CNTs-CNFs composite film; inset is SEM image with low-magnification.

with a cross-linked nanotubular structure. In our previous work (Wang et al., 2006), the pores have been reported to be mostly mesopores. The pore size distribution test result in Table 2 shows the proportion of micropore volume in the total pore volume is about 0.2% and the average pore diameter is 7.9 nm, which confirmed CNTs-CNFs films in this work are mainly composed of mesopores (2–50 nm). It is widely accepted that such a network structure permits easy access for ions to the electrode/electrolyte interface, which is crucial for a non-Faradaic capacitative electrode material (Wang et al., 2006).

Fig. 3 exhibits the typical Raman spectrum of the as-grown CNTs–CNFs. The two main modes D at $1350~{\rm cm}^{-1}$ and G at $1580~{\rm cm}^{-1}$ are observed. Generally, the G peak corresponds to the tangential stretching (E_{2g}) mode of highly oriented pyrolytic graphite, which indicates the presence of crystalline graphitic carbon in the carbon nanomaterials, while the D peak represents the disorder-induced feature due to the finite particle size effect or lattice distortion (Nemanich and Solin, 1979). The ratio of the intensity of the D peak and G peak (I_D/I_G) is related to the amount of disorder in the carbon products. The I_D/I_G ratio was 1.14. That means there are some defects in the CNTs–CNFs composite film. However, the presence of defects causes an increase in ability for accumulation of charges (Fraackowiak et al., 2002), which may be beneficial for charge transfer in the electrosorption process.

3.2. The desalination performance of MCDI

The ions were forced towards CNTs-CNFs composites electrodes from the aqueous solutions while a direct voltage was

Table 2 – Pore volume and average pore diameter of CNTs–CNFs film				
	Total pore volume (cm³/g)	Micropore volume (cm³/g)	Average pore diameter (nm)	
CNTs-CNFs film	0.1415	0.0003	7.9381	

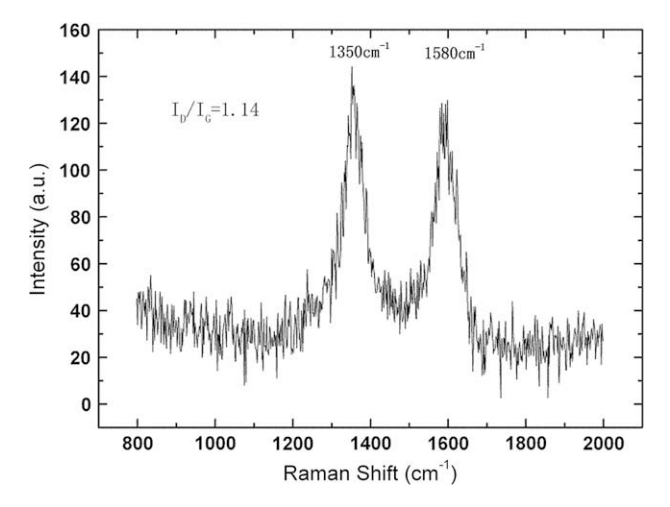


Fig. 3 - Raman spectrum of CNTs-CNFs composite film.

applied to the electrodes. The typical electrosorption experiment was conducted in a solution of NaCl that had an initial conductivity around 50 $\mu S/cm$. During mode experiments with one complete recycle, the amplitude of the applied voltage was 1.2 V. Applied voltages and conductivity transients during one charge–discharge cycle of such experiments are shown in the inset of Fig. 4. Cations and anions are adsorbed onto the electrical double layers formed at the surfaces of the CNTs–CNFs composite film electrodes during charging and they are released back into the electrolyte during discharging. This means the CNTs–CNFs composite films can be regenerated by discharging.

The electrosorption experiments of CDI and MCDI with an initial conductivity around $50\,\mu\text{S/cm}$ at $1.2\,\text{V}$ showed the similar process as shown in Fig. 4. When the voltage was applied on the electrodes, the conductivity sharply decreases with the increasing time. At the beginning of electrosorption, the salt removal of CDI with 10 pairs CNTs–CNFs electrodes in series (10-CDI) was highest among the three different devices. At about 40 min, the electrosorption of CDI with one pair of

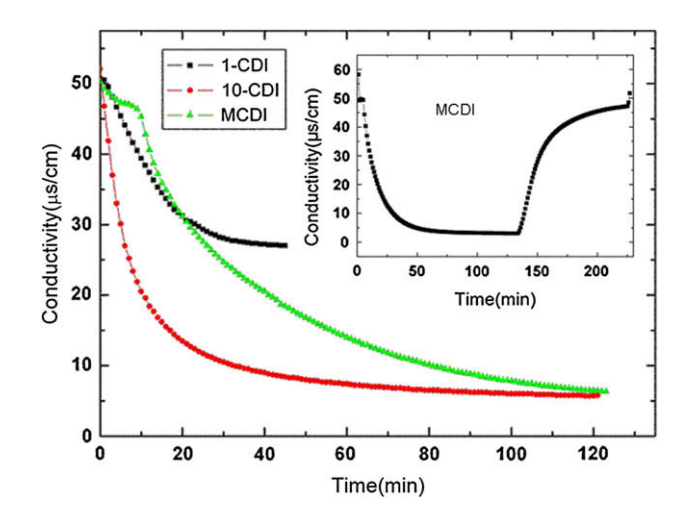


Fig. 4 – Desalination performance of MCDI, 1-CDI and 10-CDI; inset is one complete charge-discharge cycle in MCDI.

CNTs-CNFs electrodes (1-CDI) gradually reached saturation while the 10-CDI and MCDI continued to work. At about 140 and 80 min, the MCDI and 10-CDI almost did not absorb more ions, respectively. The salt removal of 1-CDI, 10-CDI and MCDI are 41.6%, 89.8% and 90.8%, respectively. Comparing with 1-CDI, MCDI exhibits much better performance. 10-CDI can remove the ions more quickly than MCDI but they have similar salt removal. If taking into account the manufacturing cost and simple structure, the MCDI is a better candidate than 10-CDI.

3.3. The electrosorption isotherm of MCDI

Several electrosorption experiments with NaCl solutions in different initial concentrations were carried out to study the electrosorption isotherms of MCDI and CDI. The initial conductivities of NaCl solutions were from 50 to 1000 μ S/cm and from 50 to 750 μ S/cm for MCDI and 1-CDI, respectively. A direct voltage of 1.2 V was applied. Fig. 5 shows the electrosorption isotherm of MCDI and 1-CDI (inset). As shown in the figure, they have the similar electrosorption isotherms. When the solution was very dilute, the adsorbed NaCl amount inclines to zero. The removal amount of NaCl increased as the initial concentration was raised, which was due to the enhanced mass transfer rate of ions inside the micropores and reduced overlapping effect by higher concentration of solution (Purdom, 1980). Langmuir isotherm (2) and Freundlich isotherm (3) models were used to fit the experimental data,

$$q = \frac{q_{\rm m}K_{\rm L}C}{1 + K_{\rm L}C} \tag{2}$$

$$q = K_F C^{1/n} \tag{3}$$

where C is the equilibrium concentration (mmol/L), q is the amount of adsorbed NaCl (in micromoles per gram of CNTs–CNFs film), $q_{\rm m}$ is the maximum adsorption capacity corresponding to complete monolayer coverage. Table 3 shows the determined parameters and regression coefficients R^2 , K_L and K_F of Langmuir and Freundlich isotherms in MCDI and 1-CDI, respectively. The regression coefficients R^2 of Langmuir and

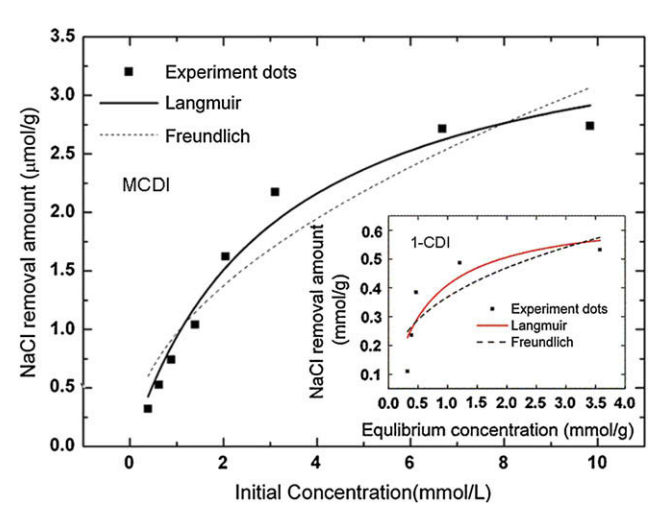


Fig. 5 - Adsorption isotherms for MCDI and CDI (inset).

	able 3 – Parameter determined from various isotherms n NaCl solutions for MCDI and CDI			
Isotherm	Model equation	Parameter	Value (MCDI)	Value (1-CDI)
Langmuir	$q = \frac{q_{\rm m} K_L C}{1 + K_L C}$	q _m K _L R ²	3.82 0.33 0.97	0.51 0.44 0.99
Freundlich	$q = K_F C^{1/n}$	K _F n R ²	0.97 1.99 0.91	0.66 1.62 0.78

Freundlich isotherms in MCDI are 0.97 and 0.91 while in 1-CDI are 0.99 and 0.78. The $q_{\rm m}$ values calculated by the Langmuir equation are 3.82 and 0.51 mmol/g by MCDI and 1-CDI, respectively, indicating the electrosorption capacity of MCDI is higher than that of 1-CDI which is consistent to the results in Fig. 4. From Fig. 5, it can be seen that the Langumuir isotherm better describes the experimental data for both of the two systems, which means that although ion-exchange membranes were introduced in MCDI system, the electrosorption of CNTs–CNFs electrode in MCDI still follows monolayer adsorption. The result also shows that the better desalination performance of MCDI than that of 1-CDI is due to the minimized ion desorption during electrosorption not to the change in adsorption behavior.

3.4. The effect of electric field on MCDI

Fig. 6 shows conductivity transients in NaCl solution during batch-mode experiments at six different applied voltages: 0.6, 0.8, 1.0, 1.2, 1.4 and 1.6 V by MCDI system, respectively. All the charge processes are carried out for 50 min. In the potential range from 0.6 to 1.6 V, the salt recovery increased from 43.9% to 93.5%. As expected, the greater the cell voltage is, the greater ion removal amount is achieved. Nevertheless, when the voltage is increased from 1.4 to 1.6 V, the salt removal does not increase. Hydrolysis of water is not found when the voltage between the two electrodes is more than 1.2 V because

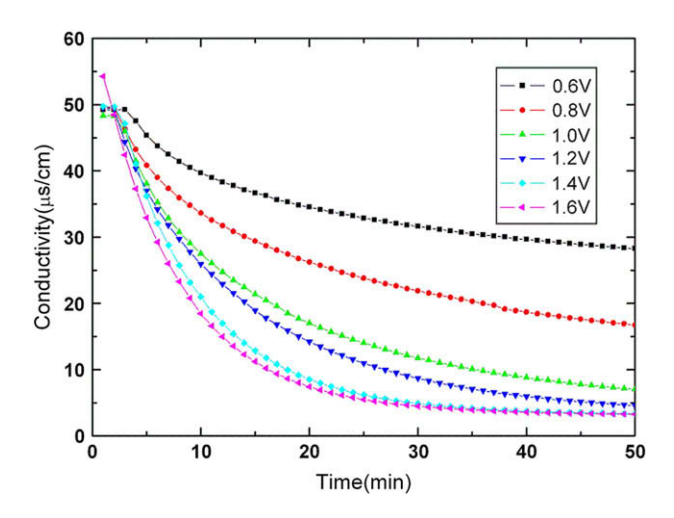


Fig. 6 – Effect of different voltage on electrosorption in NaCl solutions by MCDI.

Table 4 – Comparison of electrosorption between CNTs–							
CNF	s MCDI	and ACC MCD					

	Electrodes	Initial	Final	Salt	Electrode
		conductivity	conductivity	removal	area
		(μS/cm)	(μS/cm)	(%)	(m^2)
	ACC MCDI	1020	698	32	0.5
	CNTs-CNFs MCDI	994	684	31	0.08

of the existence of large resistance in the whole circuit (Show and Imaizumi, 2007). With respect to commercial practice, energy consumption needs to be considered in our device. Hence, taking both the salt removal and the energy consumption into account, the optimum direct voltage used in MCDI system is 1.2 or 1.4 V.

When the applied voltage is 1.2 V, the comparative results of the salt removal between the CNTs-CNFs MCDI in our experiment and activates carbon cloth (ACC) MCDI reported by Lee et al. (2006) in NaCl solutions with the same initial concentration are shown in Table 4. The CNTs-CNFs MCDI shows a similar desalination performance as ACC MCDI although electrode area in CNTs-CNFs MCDI is much smaller than that in ACC MCDI.

4. Conclusion

- A low temperature and low pressure CVD system has been used to fabricate large area CNTs-CNFs composite film electrode for electrosorption application. The characterization and electrosorption of CNTs-CNFs composite films are investigated. The CNTs-CNFs composite film shows optimal network morphology.
- The electrosorption behaviors of MCDI and CDI were studied. MCDI exhibits a much higher salt removal than 1-CDI and a similar desalination performance to 10-CDI but MCDI has simpler structure and lower cost.
- The electrosorption isotherms of MCDI and CDI show both of them follow Langmuir adsorption, indicating no change in adsorption behavior when ion-exchange membranes are introduced into CDI system. The better desalination performance of MCDI than that of CDI is mainly due to the minimized ion desorption during electrosorption.
- The CNTs-CNFs MCDI shows a similar desalination performance to ACC MCDI although electrode area in CNTs-CNFs MCDI is much smaller than that in ACC MCDI.

Acknowledgments

This work was supported by Special Project for Nanotechnology of Shanghai (No. 0752nm011), Applied Materials Shanghai Research & Development Fund (No. 07SA12),

Shanghai Natural Science Foundation (No. 07ZR14033), and Program for Chang Jiang Scholars and Innovative Research Team in University.

REFERENCES

- Fang, B., Binder, L., 2006. A modified activated carbon aerogel for high-energy storage in electric double layer capacitors. J. Power Sources 163, 616–622.
- Fraackowiak, E., Jurewicz, K., Szostak, K., Delpeux, S., Beguin, F., 2002. Nanotubular materials as electrodes for supercapacitors. Fuel Process. Technol. 77, 213–219.
- Gabelich, C.J., Tran, T.D., Suffet, I.H., 2002. Electrosorption of inorganic salts from aqueous solution using carbon aerogels. Environ. Sci. Technol. 36, 3010–3019.
- Gao, Y., Pank., L., Zhang, Y.P., Chen, Y.W., Sun, Z., 2007. Electrosorption of $FeCl_3$ solution with carbon nanotubes and nanofibres film electrodes grown on graphite substrates. Surf. Rev. Lett. 14, 1033–1037.
- Hou, C.H., Liang, C.D., Yiacoumi, S., Dai, S., Tsouris, C., 2006. Electrosorption capacitance of nanostructured carbon-based materials. J. Colloid Interface Sci. 302, 54–61.
- Hwang, S.W., Hyun, S.H., 2004. Capacitance control of carbon aerogel electrodes. J. Non-Cryst. Solids 347, 238–245.
- Johnson, A.M., Newman, J.J., 1971. Desalting by means of porous carbon electrodes. J. Electrochem. Soc. 118, 510–519.
- Lee, J.B., Park, K.K., Eum, H.M., Lee, C.W., 2006. Desalination of a thermal power plant wastewater by membrane capacitive deionization. Desalination 196, 125–134.
- Matlosz, M., Newman, J., 1986. Experimental investigation of a porous carbon electrode for the removal of mercury from contaminated brine. J. Electrochem. Soc. 133, 1850–1859.
- Nemanich, R.J., Solin, S.A., 1979. First-and second-order Raman scattering from finite-size crystals of graphite. Phys. Rev. B 20, 392–401.
- Oh, H.J., Lee, J.H., Ahn, H.J., Jeong, Y., Kim, Y.J., Chi, C.S., 2006. Nanoporous activated carbon cloth for capacitive deionization of aqueous solution. Thin Solid Films 515, 220–225.
- Pekala, R.W., Farmer, J.C., Alviso, C.T., Tran, T.D., Mayer, S.T., Miller, J.M., Dunn, B., 1998. Carbon aerogels for electrochemical applications. J. Non-Cryst. Solids 225, 74–80.
- Purdom, P.W., 1980. In: Environmental Health, second ed. Academic Press, New York.
- Qi, D.D., Zou, L., Hu, E., 2007. Electrosorption: an alternative option for desalination. Res. J. Chem. Environ. 11, 92–95.
- Qu, D.Y., Shi, H., 1998. Studies of activated carbons used in double-layer capacitors. J. Power Sources 74, 99–107.
- Show, Y., Imaizumi, K., 2007. Electric double layer capacitor with low series resistance fabricated by carbon nanotube addition. Diam. Relat. Mater. 16, 1154–1158.
- Wang, X.Z., Li, M.G., Chen, Y.W., Cheng, R.M., Huang, S.M., Pan, L. K., Sun, Z., 2006. Electrosorption of ions from aqueous solutions with carbon nanotubes and nanofibers composite film electrodes. Appl. Phys. Lett. 89, 053127-4.
- Welgemoed, T.J., Schutte, C.F., 2005. Capacitive Deionization technology™: an alternative desalination solution. Desalination 183, 327–340.
- Xu, P., Drewes, J.E., Heil, D., Wang, G., 1983. Treatment of brackish produced water using carbon aerogel-based capacitive deionization technology. Water Res. 42, 2605–2617.
- Zou, L.D., Li, L.X., Song, H.H., Morris, G., 2007. Using mesoporous carbon electrodes for brackish water desalination. Water Res. 42, 2340–2348.